JBIC (1999) 4:166–170

ORIGINAL ARTICLE

Louise A. Evans · Rebeca Alvarez

Characterization of the calcium biomineral in the radular teeth of *Chiton pelliserpentis*

Received: 18 September 1998 / Accepted: 22 December 1998

Abstract The radula in a group of molluscan invertebrates, the chitons (Polyplacophora), is a ribbon-like apparatus used for feeding and which bears a series of distinctive mineralized teeth called the major lateral teeth. While some chiton species deposit only iron biominerals in these teeth, many others deposit both iron and calcium. In this study, the calcium biomineral in the teeth of one of the latter types of species, the Australian east-coast chiton, *Chiton pelliserpentis*, has been isolated and examined for the first time. Spectroscopic and crystallographic techniques have identified the biomineral as a carbonate-substituted apatite with significant fluoride substitution also likely. Fourier-transform infrared and laser Raman spectroscopy indicated that the carbonate content was less than that of either bovine tibia cortical bone or human tooth enamel. X-ray diffraction analysis showed the biomineral to be poorly crystalline due to small crystal size and appreciable anionic substitution. The lattice parameters were calculated to be $a = 9.382$ Å and $c = 6.883$ Å, which are suggestive of a fluorapatite material. It is postulated that structural and biochemical differences in the tooth organic matrix of different chiton species will ultimately determine if the teeth become partly calcified or iron mineralized only.

Key words Molluscs · Chiton radula · Carbonated apatite · Laser Raman spectroscopy · Fourier transform infrared spectroscopy

L.A. Evans (✉) · R. Alvarez
Department of Chemistry, Materials and Forensic Science
University of Technology, Sydney, PO Box 123, Broadway
New South Wales 2007, Australia
e-mail: louise.evans@uts.edu.au
Tel.: +61-2-95141727
Fax: +61-2-95141628

Introduction

The presence of calcium phosphate biominerals in invertebrate tissues is quite rare, these systems being dominated by calcium carbonate (e.g. molluscan shells and coral). However, calcium phosphate is known to occur in some brachiopod shells [1] and in the teeth of certain chiton species [2]. This paper will focus on the biomineralization processes occurring in chitons (Mollusca: Polyplacophora). Chitons are marine organisms whose microscopic mineralized teeth are borne on a radula or tongue (Fig. 1). The minerals are deposited onto a preformed organic matrix, comprising mostly α-chitin together with smaller amounts of phosphorylated proteins [3, 4]. In the early stages of mineralization, iron biominerals (ferrihydrite, $5Fe_2O_3.9H_2O$; magnetite, Fe_3O_4; and lepidocrocite, γ-FeO.OH) are deposi-

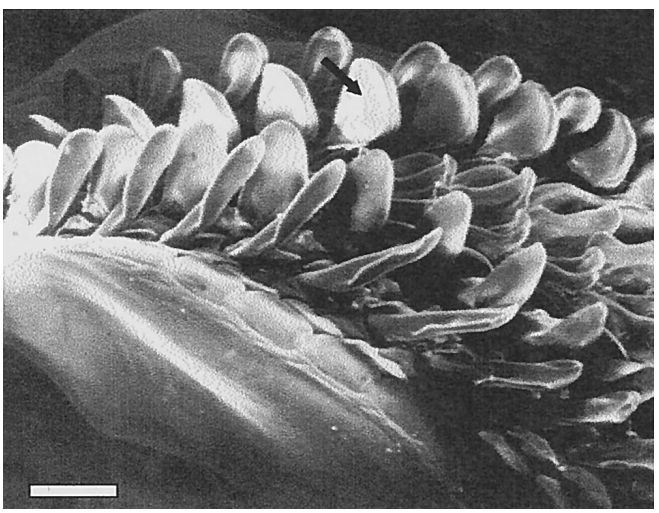

Fig. 1 Scanning electron micrograph illustrating the diversity of teeth arranged on the chiton radula. The mineralized major lateral teeth (arrowed) are the largest of the different tooth structures. The radular membrane is clearly evident in the lower left-hand region. *Scale bar* 200 μm

ted in the posterior (cutting) region of the tooth. At later stages of development the anterior region becomes infilled with either an amorphous ferric phosphate material [5] or an apatite mineral [2]. In species which deposit the latter material, the iron biominerals are, generally speaking, associated with small amounts of organic material; however, the calcium mineral is deposited onto highly ordered rope-like strands of α-chitin (a polysaccharide), which give the tooth structure tensile strength and flexibility [3]. Iron and calcium biominerals are thus found in architecturally discrete regions of the tooth which are chemically and structurally dissimilar. The teeth along the radula occur in sequential stages of development, ranging from organic only, followed by iron mineralized, through to both iron and calcium mineralized. Thus the chiton radular system presents an unusual opportunity to study the maturation of the mineralization processes occurring in Nature.

Previous studies of chiton tooth biominerals have tended to focus on the iron biominerals, particularly the magnetite capping of the mineralized (major lateral) teeth [6–9]. Because of the complications caused by the presence of iron biominerals and large amounts of organic material, only a few papers have examined the calcium biomineral. These studies have suggested that the calcium biomineral is either francolite, a carbonated fluorapatite [2], or dahllite, a carbonated hydroxyapatite [10], or a carbonate and fluoride substituted apatite material [11]. The aim of the work reported here was to characterize the calcium biomineral in the teeth of *Chiton pelliserpentis*, a species never examined before and which is found on intertidal rocks along the south-east coast of the Australian continent. Because this biomineral is deposited in the tissue towards the final stages of tooth development, it was chemically isolated from the iron biominerals and the organic components before being characterized by the combined techniques of infrared spectroscopy, laser Raman spectroscopy and X-ray diffraction analysis.

Materials and methods

C. pelliserpentis specimens were collected from intertidal rocks near the Sydney metropolitan area (latitude 34°S, longitude 151°E) and their radulae dissected out. The radulae were cleaned briefly in 2% w/v NaOCl to remove overlaying cellular debris. To preclude the presence of any precursor calcium-containing compounds, such as amorphous calcium phosphate [10], only fully mature segments were used (approximately last 25% of radular tissue).

For isolation of the calcium biomineral from the iron biominerals, radular segments were treated according to the method of Evans et al. [11]. Briefly, this method involves the reduction of iron(III) using sodium dithionite followed by complexation with 2,2′-bipyridyl. Removal of iron from the tissue may be confirmed by the formation of the intensely coloured bisbipyridyliron(II) complex in solution. Note that this method has been shown not to affect apatite materials. To remove the organic material, the iron-demineralized radular segments were then treated with NaOCl solution according to the method of Weiner and Price [12].

The calcium biomineral thus obtained was analysed by Fourier transform infrared (FT-IR) spectroscopy by preparing 13-mm pellets (2 mg sample/200 mg KBr), which were mounted in a BIO-RAD FTS 7 spectrometer attached to a SPC 3200 workstation. Raman spectra were obtained using a Dilor-XY modula Raman spectrometer with 514.52 nm radiation from an argon laser source. The source laser power used was 50 mW, with integration times of 100 s.

X-ray diffraction (XRD) analyses were obtained with a Siemens D500 diffractometer using Cu-K_α radiation generated at 40 kV and 30 mA. Diffraction patterns were recorded in the 2θ range 20 to 60°, with a scanning speed of 0.01°/s. A silica standard was used to calibrate the instrument. Lattice parameters were calculated from the (410) and (300) reflections (*a*-axis) and from the (004) and (002) reflections (*c*-axis) using a hexagonal indexing system [13].

Reference material for FT-IR, laser Raman and XRD analyses were obtained from the following sources: human tooth enamel was prepared from caries-free adult human teeth using a tetrabromoethane flotation method (d 2.7 g cm^{-3}) to separate enamel from dentine [14]; bovine tibia cortical bone was prepared

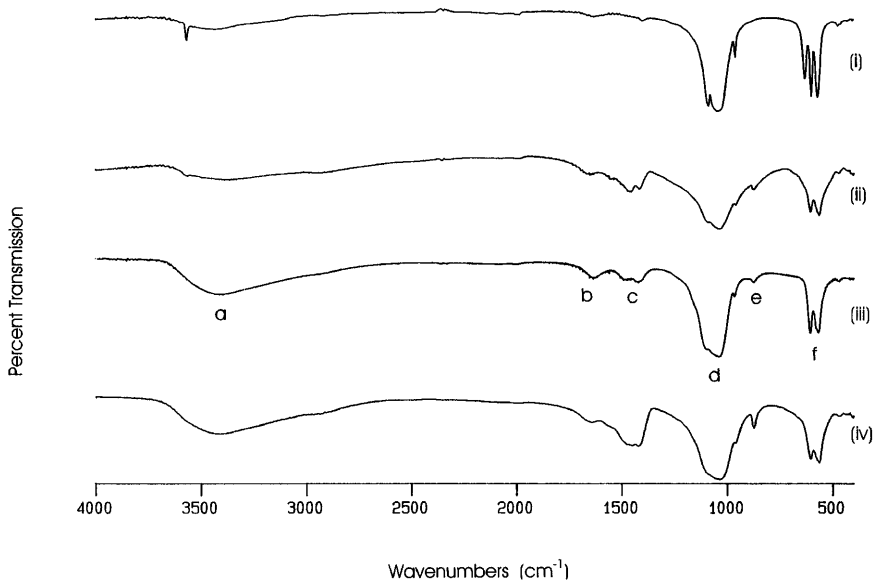

Fig. 2 Fourier transform infrared spectra from (*i*) stoichiometric synthetic hydroxyapatite, (*ii*) human tooth enamel, (*iii*) chiton tooth biomineral, and (*iv*) bovine tibia cortical bone. Absorption bands labelled *a–f* are due to the following groups: *a* H_2O, *b* H_2O, *c* CO_3, *d* PO_4, *e* CO_3, *f* PO_4. Note that the sharp band at 3572 cm^{-1} clearly evident in (*i*) and less obvious in (*ii*) is due to an OH stretching vibration

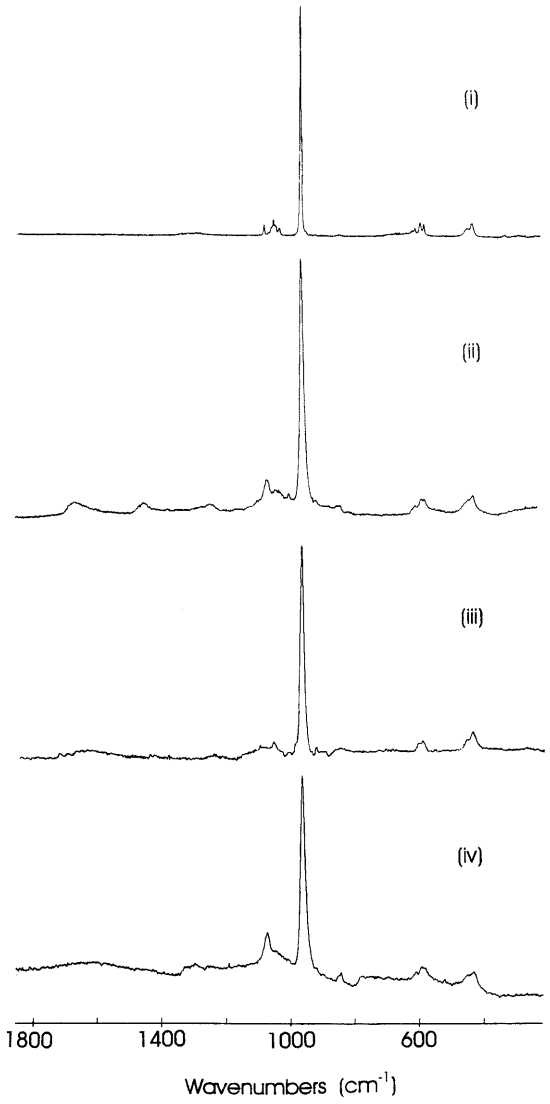

Fig. 3 Laser Raman spectra of (*i*) stoichiometric synthetic hydroxyapatite, (*ii*) human tooth enamel, (*iii*) chiton tooth biomineral, and (*iv*) bovine tibia cortical bone. Note that the mercury green line appearing at 1122.7 cm^{-1} in all spectra has been omitted for clarity

using NaOCl solution to remove organic components [12]; and synthetic high-temperature stoichiometric hydroxyapatite (HAP) was prepared using the solid state method of Nelson and Williamson [14].

Results

The FT-IR spectrum of chiton biomineral obtained following its chemical isolation consisted of bands due to the following groups: CO_3, PO_4 and H_2O (Fig. 2) and showed similarities to the biogenically derived reference materials of bovine tibia cortical bone and human tooth enamel. For synthetic HAP, the carbonate v_2 and v_3 vibrational modes occurring at about 875 cm^{-1} and 1500–1400 cm^{-1}, respectively, were greatly reduced when compared to the biogenic samples. None of the samples showed any absorption in the 720–700 cm^{-1} (CO_3 ν_4) range.

All apatite samples (including synthetic HAP) showed bands due to PO_4 groups: ν_1 at about 960 cm^{-1}, triply degenerate ν_3 bands in the 1100–1000 cm^{-1} range and ν_4 bands between 600 and 550 cm^{-1}. The PO_4 ν_2 bands were only just visible between 480 and 460 cm^{-1}. The broad absorption band from 3600 to 3000 cm^{-1} and a second band at 1640 cm^{-1} in all the spectra correspond to strongly adsorbed water on the surface of apatite crystals [15].

Although not present in the chiton and bone spectra, the OH stretching band at 3572 cm^{-1} was clearly visible in the spectrum of synthetic HAP and weakly visible in the spectrum of enamel. The OH librational band was only visible, however, in the spectrum of stoichiometric HAP at 634 cm^{-1}. Interestingly, the FT-IR spectrum of chiton apatite showed evidence of a distinct shoulder at 575 cm^{-1} which has been attributed to F or Cl substitution for OH [1].

The laser Raman spectrum of all samples was dominated by a strong band at 960 cm^{-1}, corresponding to the totally symmetric ν_1 stretching mode of the phosphate tetrahedron [14]. Bands corresponding to other phosphate vibrational modes were visible at 480–400 cm^{-1} (ν_2), 680–560 cm^{-1} (ν_4) and 1100–1000 cm^{-1} (ν_3). The symmetric CO_3 ν_1 band was clearly evident in the spectra of enamel and bovine tibia at 1070 cm^{-1}, superimposed on the phosphate ν_3 bands (Fig. 3). Only the synthetic material showed the hydroxyl stretching band at 3572 cm^{-1}. All biological samples showed evidence of low background noise due to fluorescence caused by residual organic matrix components.

The X-ray diffraction pattern of isolated chiton biomineral was characteristic of a poorly crystalline apatite material (Fig. 4). The lattice constants of *C. pelliserpentis* apatite were calculated to be $a = 9.382$ (± 0.005) Å and $c = 6.883$ (± 0.005) Å.

Discussion

The work reported here on *C. pelliserpentis* represents the first major study of the calcium biomineral in the teeth of a species inhabiting the south-east coastline of the Australian continent. In this investigation, the calcium biomineral has been successfully isolated from the other (iron) biominerals and subsequently characterized. Thus, the calcium biomineral from *C. pelliserpentis* has been shown to be a carbonate-substituted apatite, as discussed below.

Comparison of the FT-IR spectra of synthetic HAP and the biogenic apatites showed distinct differences, the most obvious being the greatly increased intensity of the CO_3^{2-} ν_3 bands for biogenic apatites between 1500 and 1415 cm^{-1}. A smaller intensity band at about 875 cm^{-1}, present only in the biogenic apatites, is also due to carbonate (ν_2). Hence the presence or the ab-

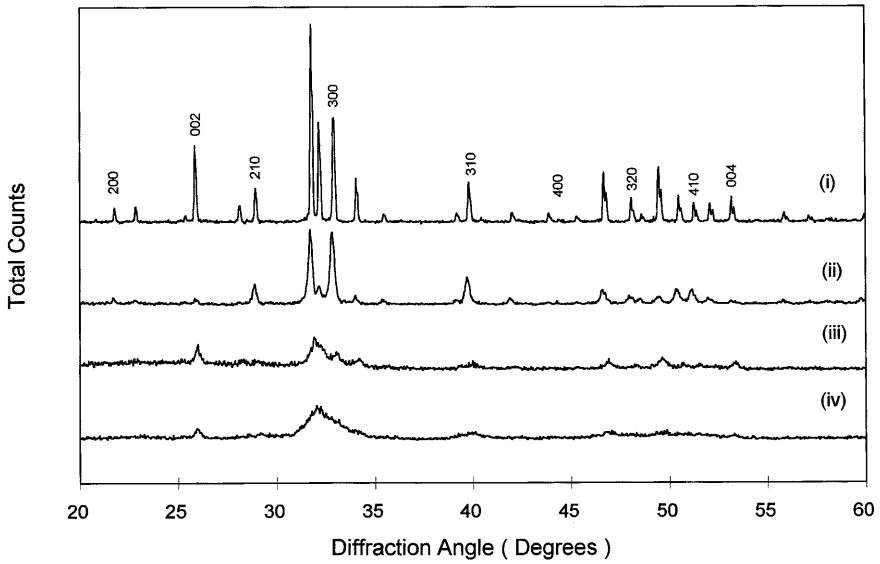

Fig. 4 X-ray diffraction patterns of (*i*) stoichiometric synthetic hydroxyapatite, (*ii*) human tooth enamel, (*iii*) chiton tooth biomineral, and (*iv*) bovine tibia cortical bone. The differences in the relative peak intensities in (*ii*) are due to a preferred crystal orientation in the case of the enamel specimen

sence of these bands will immediately confirm or preclude the presence of carbonate. Note that the absence of a carbonate ν_4 band in the 720–700 cm^{-1} region has been shown to rule out the presence of carbonate as a separate calcium carbonate phase [16]. Comparison of the relative intensities of the carbonate bands suggests that the extent of carbonate substitution would be in the order: bone > enamel > chiton. Since values of approximately 2.5% w/w carbonate have been reported for human tooth enamel [17], this imposes an upper limit on the degree of carbonate substitution in the chiton sample.

The other noticeable difference between synthetic HAP and the biogenic apatites was in the appearance of the hydroxyl bands at 3572 cm^{-1} and 634 cm^{-1}. Since the first band was not apparent in the chiton and bone spectra, these samples could not be identified as HAP based on IR spectroscopy alone. Note that the absence of the second hydroxyl band in all biogenic samples has been attributed to hydroxyl ion deficiencies in the structure of carbonated apatites [14]. The distinct shoulder appearing in the 575 cm^{-1} phosphate ν_4 band of the chiton spectrum has been seen previously in another chiton species, *Acanthopleura hirtosa* [11]. In this study the shoulder was attributed to the presence of F substituting for OH. Note that this study also suggested that the "switch" in the relative intensities of the C-O 1450 cm^{-1} and 1510 cm^{-1} bands when compared to human enamel is characteristic of a carbonate and fluoride containing apatite rather than carbonated apatite alone.

Laser Raman spectral results indicated that the material isolated from *C. pelliserpentis* is a calcium phosphate material, as evidenced by the position of the strong band at 960 cm^{-1} [18]. In addition, the Raman results substantiate the IR supposition that the chiton biomineral is less carbonated than enamel or bone since the carbonate ν_1 band for chiton was greatly weakened relative to these samples.

The broadness of the XRD peaks is an indication of the crystallinity of the sample which, in turn, is a function of either crystal size or degree of substitution since either phenomenon will disrupt the long range regularity of the crystal structure. Thus XRD peak broadening for the chiton sample indicates a material which is similar in crystallinity to bovine tibia but far less crystalline than either human tooth enamel or synthetic stoichiometric HAP. It is possible, however, that the diffuse appearance of the XRD peaks for chiton is due not only to the poor crystallinity of the sample, but also to the small amount of material available for analysis. In addition, the presence of residual organics will cause broadening of the peaks.

The chiton lattice parameters reported here are shorter in the *a*- and very similar for the *c*-axis when compared to human tooth enamel ($a = 9.441$, $c = 6.882$ Å). Studies by LeGeros et al. [1, 16] have found that carbonate substitution results in a shortening of the *a*-axis and expansion in the *c*-axis and that fluoride substitution causes a contraction in the *a*-axis but does not affect the *c*-axis. Thus it is possible to explain these differences in terms of a similar carbonate but increased fluoride substitution for chiton when compared to enamel. We note that the lattice parameters reported here for chiton apatite are very close to those reported for fluorapatite [1] and that fluorapatite is the most common of the naturally occurring apatites [19].

The area of the tooth in which the calcium biomineral is deposited is a vital structural component since it is the combination of organic and inorganic components here which give the tooth mechanical properties of tensile strength and flexibility. Characterization of the calcium biomineral in *C. pelliserpentis* shows great resemblance to that of the Western Australian species, *A. hirtosa* [11]. The finding that both these species deposit a carbonate-substituted apatite with possible Cl or F substitution for OH is suggestive of similar biomineraliza-

tion processes occurring within these species. However, it must be recalled that in other chiton species the calcium biomineral is replaced by an amorphous ferric phosphate and that differences in the structural organization of the organic matrix are also apparent [20].

In species which deposit calcium, it has been postulated that a specialized dense meshwork of organic fibres running longitudinally through the tooth cusp are responsible for preventing the passage of iron into the anterior region of the tooth [21]. This keeps nucleation sites in this region free to bind Ca^{2+} when this ion is delivered to the mineralization front at later stages of tooth development.

We propose that, because species depositing only iron phases do not possess the same structural organization of organic matrix fibres, the iron delivered to the mineralization front can travel freely through the tooth and is thus deposited throughout. Differences in the actual iron phase deposited are probably due to localized differences in the oxidative properties and degree of phosphorylation of the organic matrix. A biochemical study comparing the differences between the organic matrices of a calcium-containing species and an "iron only" species will further elucidate the divergent biomineralization processes occurring in chiton teeth.

Acknowledgements We thank R. Tassone for assistance in collection of chiton specimens and preparation of reference materials, together with Dr. R. Ashby and R. Wuhrer for their excellent technical assistance. Funding from a UTS Internal Research Grant is gratefully acknowledged.

References

1. LeGeros RZ, Pan CM, Suga S, Watabe N (1985) Calcif Tissue Int 37:98–100
2. Lowenstam HA (1967) Science 156:1373–1375
3. Evans LA, Macey DJ, Webb J (1990) Philos Trans R Soc Lond B 329:87–96
4. Evans LA, Macey DJ, Webb J (1991) Mar Biol 109:281–286
5. Lowenstam HA, Weiner S (1989) On biomineralization. Oxford University Press, Oxford
6. Van der Wal P, Videler JJ, Havinga P, Pel R (1989) In: Crick RE (ed) Origin, evolution and modern aspects of biomineralization in plants and animals. Plenum Press, New York, pp 153–166
7. Van der Wal P (1991) In: Frankel RB, Blakemore RP (eds) Iron biominerals. Plenum Press, New York, pp 221–229
8. Kim K-S, Macey DJ, Webb J, Mann S (1989) Proc R Soc Lond B 237:335–346
9. Lee AP, Webb J, Macey DJ, van Bronswijk W, Savarese AR, de Witt GC (1998) JBIC 3:614–619
10. Lowenstam HA, Weiner S (1985) Science 227:51–53
11. Evans LA, Macey DJ, Webb J (1992) Calcif Tissue Int 51:78–82
12. Weiner S, Price PA (1986) Calcif Tissue Int 39:365–375
13. Cullity BD (1978) Elements of x-ray diffraction, 2nd edn. Addison-Wesley, Reading, Mass, pp 324–349
14. Nelson DGA, Williamson BE (1982) Aust J Chem 35:715–727
15. Posner AS, Betts F, Blumenthal NC (1979) In: Simmons DJ, Kunin AS (eds) Skeletal research. Academic Press, New York, pp 167–192
16. LeGeros RZ, LeGeros JP, Trautz OR, Klein E (1970) Dev Appl Spectrosc 7:3–12
17. Zapanta-LeGeros R (1965) Nature 206:403–404
18. Sauer GR, Zunic WB, Durig JR, Wuthier RE (1994) Calcif Tissue Int 54:414–420
19. Hurlbut CS (1971) Dana's manual of mineralogy, 18th edn. J Wiley, New York
20. Macey DJ, Brooker LR, Webb J, St Pierre TG (1997) Acta Zool (Stockh) 77:287–294
21. Evans LA, Macey DJ, Webb J (1994) Acta Zool (Stockh) 75:75–79